atmosphere

MDPI

Article

Impacts of a Prescribed Fire on Air Quality in Central New Mexico

Christian M. Carrico * and Jaimy Karacaoglu †

New Mexico Institute of Mining and Technology, 801 Leroy Place, Socorro, NM 87801, USA
* Correspondence: kip.carrico@nmt.edu; Tel.: +1-575-835-5165
† Current address: Trinity Consultants, 9400 Holly Avenue NE, Building 3, Suite B, Albuquerque, NM 87122, USA.

Abstract: A short-duration but high-impact air quality event occurred on 28 November 2018 along the Rio Grande Valley of New Mexico. This fire occurred outside the typical wildfire season, and greatly impacted the air quality in Socorro, NM, and the surroundings. Measurements were taken during the event using an aerosol light scattering technique (integrating nephelometer) and a particulate mass concentration monitor (DustTrak PM optical monitor). The instruments sampled the ambient air during the event on the campus of the New Mexico Institute of Mining and Technology in Socorro, New Mexico. The peak values on a 5-min basis of light scattering and the PM mass concentration reached 470 Mm^{-1} and 270 $\mu g/m^3$, respectively. We examined the meteorological context of the event using local meteorological data and back trajectories using the NOAA HYSPLIT model to determine atmospheric transport and possible sources. Several fires, both prescribed and wildfires, occurred in the region including a prescribed burn at Bosque del Apache National Wildlife Refuge (17 km south-southeast of the receptor site). The data suggest that the prescribed burn at Bosque del Apache was the dominant contributor due to transport evidence and the event's narrow spatiotemporal extent. The increasing importance of restoring ecosystem function using prescribed fire in wildland fire management will likely lead to more frequent air quality impacts and sets up policy tradeoffs that require a balance between these public goals. This study examines the evidence of the effects of a prescribed fire in a protected wildland area impacting the air quality in a nearby populated area.

Keywords: aerosols; biomass burning; prescribed fire; visibility; climate forcing; $PM_{2.5}$

Citation: Carrico, C.M.; Karacaoglu, J. Impacts of a Prescribed Fire on Air Quality in Central New Mexico. *Atmosphere* **2023**, *14*, 316. https://doi.org/10.3390/atmos14020316

Academic Editor: Patricia K. Quinn

Received: 27 December 2022
Revised: 30 January 2023
Accepted: 31 January 2023
Published: 5 February 2023

1. Introduction

The smoke emitted by regional wildland fires has a significant and growing impact on air quality in the western United States [1,2], including New Mexico. Smoke aerosol emissions also have significant interplay with climate forcing [3]. For decades, western U.S. wildfires have increased in size and severity due to changes in climate, such as longer, hotter summers extending the fire season [4]. The climate change impacts on landscapes, including extreme weather events, have important implications for the biosphere in terms of both natural landscapes and agricultural production [5]. Besides climatic changes, increasing human activities, including both fire ignition and fire suppression activities, are also important drivers of changes to fire ecology [6].

The aerosols from wildfires and prescribed fires contain both particulate matter and gas-phase pollutants [7]. $PM_{2.5}$ (particulate matter with a diameter less than 2.5 µm) penetrates deeply into human lungs, causing substantial pulmonary damage [8]. $PM_{2.5}$ also reduces atmospheric visibility by scattering and absorbing solar radiation [9]. The latter effects also make $PM_{2.5}$ relevant to regional climate changes [10].

To mitigate wildfire impacts, various forest management techniques have been implemented including prescribed burning. Prescribed burns are meant to reduce hazardous fuel loads, restore woodlands, and manage landscapes [11]. An integrated, multi-tool fire management strategy helps reduce the severity of impacts from accelerating uncontrolled wildfires [6]. It also has the potential to mitigate air quality impacts by choosing where, when, how, and how large the prescribed fire, as contrasted with uncontrolled wildfire events. However, it should be noted that prescribed fire is only one key tool in a multi-pronged approach to wildfire response; thisalso includes adapting to accelerating fire impacts including air pollution [12].

Though the number of wildfires in the United States has declined since 1980, the fire size and acreage burned with each fire have increased dramatically (www.nifc.gov, accessed 19 December 2022). The gas-phase species that are emitted in biomass burning include carbon monoxide (CO), carbon dioxide (CO_2), nitrogen oxides (NO_x), and volatile organic compounds (VOCs) [13,14]. The particulate matter emitted includes both organic carbon and elemental carbon [15]. Depending on the fuel combusted, significant primary emissions of inorganic ions may occur as well [14,16]. The emissions of both trace gases and particulate matter can influence the overall solar radiation that is absorbed by the Earth's atmosphere during fire events. This can cause climate effects within the region including suppression of clouds and precipitation, enhancements of climate anomalies, and a reduction in surface temperature [17].

In the last two decades, the importance of prescribed burning has become clear for ecosystem management as well as air quality impacts [1,12,18]. Both public and firefighter health exposures to biomass smoke are significant during such events [8,19]. Though often difficult to measure due to their discrete nature, prescribed fires have impacted air quality in rural and urban areas around the world [20,21]. Furthermore, the emissions of trace gases and aerosols differ from wildfire to prescribed fire [22–24]. Plume scale and dilution affect prescribed fires more than large wildfire plumes [25]. Since some aging effects happen relatively quickly (10 min scale) [26], the ~1.5 h age of the plume measured in this work would be considered neither very aged nor entirely fresh. The ambient measurements of prescribed fires in southern California showed no increase in organic aerosol over a similar timescale (5 h), indicating that volatilization due to plume dilution is at least as important as secondary organic aerosol formation [27]. Select studies have shown emission reductions in fine particles in prescribed burning vs. wildfires [22]. Thus, it is important to elucidate the properties and effects of prescribed burning as it will continue to be a critical management tool.

The overall intent of this case study is to diagnose the observed smoke properties during a haze event outside the normal wildfire season on 28 November 2018. Regional data available for $PM_{2.5}$ composition, surrounding monitoring station data, air mass back trajectories, and wind speed and direction were examined in making the case for a brief though large magnitude air quality episode from prescribed burning. This finding was unexpected, and other such events could easily be attributed to wildfires or other sources. With emerging climatic changes, the tradeoffs between needed ecosystem and air quality management will become more acute.

2. Materials and Methods

Measurements were taken on 28 November 2018 at the New Mexico Institute of Mining and Technology campus in Socorro, New Mexico (located at 34.067° N 106.907° W at an elevation of 1396 m ASL) (Figure 1). The map also shows the Interagency Monitoring of Protected Visual Environments (IMPROVE) air quality monitoring station (BOAP1) at the nearby Bosque del Apache Wilderness Area (BOAP) where data was also examined. The Rio Grande Valley runs north–south through New Mexico, passing through the study area as shown with the green strip in Figure 1.

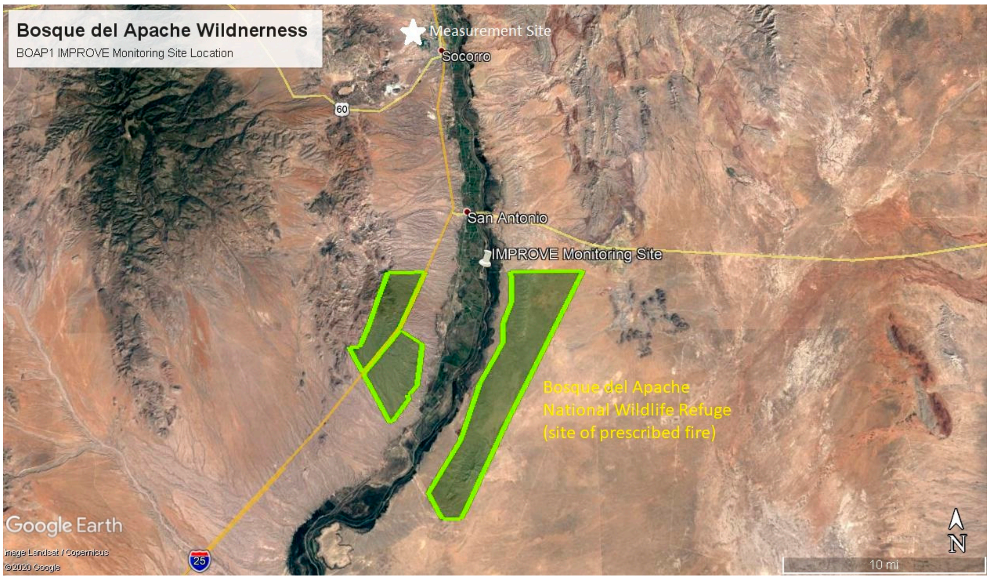

Figure 1. Location of the Bosque del Apache National Wilderness National Wildlife Refuge is demarcated in green in relation to the receptor site in Socorro, NM (Google Earth). The Interagency Monitoring of Protected Visual Environments (IMPROVE) air quality monitoring station (BOAP1) is also shown.

Continuous ambient sampling allowed the sampling of smoke events in real time with in situ measurements. A single wavelength nephelometer (Ecotech Inc., Melbourne, Australia, M9003, 520 nm) and a DustTrak Aerosol Monitor (TSI, Inc., Shoreview, MN USA, Model 8520) both sampled ambient air. The two instruments, located indoors, sampled at a height of 2 m above ground level from a common 1.25 cm stainless steel inlet line. The sampling occurred through stainless steel or other electrically conductive sampling lines with a minimum of bends to reduce particle loss. No external size cut on the inlet was possible, which was a non-ideality.

We measured 5 min particulate matter mass concentrations ($PM_{2.5}$ in $\mu g/m^3$) with a DustTrak Aerosol Monitor. The monitor sampled at a flow rate of 1.7 actual lpm as verified with an external flow standard (BIOS, DryCal). The instrument used a 780 nm laser diode and a fixed-angle 90° light scattering sensor to yield an approximate $PM_{2.5}$ with a range of 1 $\mu g/m^3$ to 100 mg/m^3 and a 24 h zero stability of ± 1 $\mu g/m^3$. Though the DustTrak instrument lacked a relative humidity (RH) measurement, with the low ambient RH and the warmer-than-ambient conditions in the instrument, this measurement was functionally 'dry' as well. The DustTrak sampled through an internal 2.5 μm-sized cut at the instrument inlet. This possibly biased the PM mass measurement lower thoughe we lacked direct sizing data on this smoke. From many past measurements in the lab and the field, fresh to even moderately aged biomass smoke was dominated by particles with diameters (D_p) ~0.1–0.4 μm [7,28,29], and the smoke sampled 17 km downwind was largely devoid of large ash particles. Thus, the measurements were functionally comparable and representative of $PM_{2.5}$ properties given the sub-micrometer fresh biomass smoke. The DustTrak was recently factory calibrated ~6 months before sampling using the default Arizona Test Dust (ATD). The smoke sampled here undoubtedly differed from ATD due to its size and optical properties, introducing an uncertainty. Zero adjustments (using HEPA filtered air) conducted both before and after the measurements were used to constrain low $PM_{2.5}$ instrument response ≤ 1 $\mu g/m^3$.

Simultaneously, we measured 5 min average particle light scattering coefficients (σ_{sp}) in inverse megameters (Mm^{-1}) with a single-wavelength integrating nephelometer (Ecotech Inc., M9003 at 520 nm). Here, we report measurements of σ_{sp} while the total light extinction (σ_{ext}) coefficient results from the sum of light scattering and absorption by particles and gases (Equation (1)):

$$\sigma_{ext} = \sigma_{sp} + \sigma_{sg} + \sigma_{ap} + \sigma_{ag}, \quad (1)$$

where σ_{ext} is the total extinction coefficient, σ_{sg} is the light scattering due to gases (Rayleigh scattering), σ_{ap} is the particle light absorption coefficient, and σ_{ag} is the gas light absorption coefficient. To calculate visual range L_v, or the distance from which an object could be distinguished from the background, the Koschmieder relationship was used, defined as $3.9/\sigma_{ext}$. Visual range estimated from σ_{sp} measured here was an upper bound as it ignores contributions from light absorption and extinction by gases.

The nephelometer sampled at a flow rate of 5 lpm. All data here, including light scattering values, were reported at as-measured conditions with no corrections to STP or for truncation losses (measuring slightly less than the entire phase function). Nephelometer truncation corrections require the size distribution or wavelength dependence to be available; here, these corrections were suspected to be quite small (~5% or less) for the fresh biomass smoke sizes sampled [30]. The nephelometer internal relative humidity (RH) over the event was RH = 12.6% ± 1.6% (mean and standard deviation during the sampling period) and was measured with a standard capacitive-type RH sensor (Vaisala, uncertainty ± 2%). This indicated approximately 'dry' conditions and negligible minimal influence of ambient RH changes (which was 19.5% ± 3.8% during the event). No additional size discrimination, sample drying, heating, filtering, denuding, or other treatment of the sample stream occurred.

The nephelometer used a 2-point calibration with CO_2 as a span gas and HEPA-filtered air as a zero gas (Table 1). The zero air was double filtered, including a HEPA filter to eliminate all particles. For a span gas, σ_{sg} was measured for which the value for CO_2 was known to be 34.87 Mm^{-1} at 520 nm and Standard Temperature (T) and Pressure (P) (STP, 273.15 K, 1013.2 hPa). The nephelometer subtracted Rayleigh scattering (scattering by gases) using real-time T and P measurements to provide particulate light scattering coefficients, σ_{sp}. The measurements were collected during a month-long student measurement lab with instrument calibration checks (no calibration adjustments required) performed approximately 2 weeks before, during the week of the event, and 2 weeks after the event (Table 1).

Table 1. Nephelometer calibration data (n = 3 calibrations before, during, and after the sampling period).

Calibration Gas	Expected Response (Mm^{-1}) *	Measured Mean (Mm^{-1}) *	Measured Standard Deviation (Mm^{-1})
CO_2 Span Gas	19.4	18.6	3.2
Particle-Free Air	0	0.0	−0.4

* Rayleigh scattering was subtracted from these values, and measurements were adjusted to local pressure and temperature (855 hPa, 295 K), both to match the nephelometer output.

The Hybrid Single-Particle Lagrangian Integrated Trajectory model (HYSPLIT), developed by the National Oceanic and Atmospheric Administration (NOAA), is a useful tool for back trajectory modeling based on meteorological data [31]. The model simulations were conducted through the Real-Time Environmental Applications and Display System (READY) [32]. The meteorological data selected in HYSPLIT runs came from the NOAA High-Resolution Rapid Refresh data on a 3 km grid. Back trajectories assumed isentropic vertical motion. Air masses arriving at the sampling site at a receptor height of 500 m above ground level were tracked backward for 24 h. Six arrival times were simulated during the event on 28 November 2018 at 23:00 UTC (16:00 MST) and on each hour back until 17:00 UTC (11:00 MST). During each of the six hours of the smoke event, the back trajectory thus traced the air mass movement backwards in time for 24 h. A local National Weather

Service meteorological station, located at 34.066° N 106.901° W (~0.5 km from the sampling site) provided winds data (20 min) for analysis of wind direction and speed to further investigate transport.

3. Results and Discussion

The measured particulate light scattering coefficients ranged from ~0 < σ_{sp} < 470 Mm^{-1} (5 min averages) as seen in Figure 2. The smoke event began at approximately 11:30 MST (local standard time) and persisted until 15:30 MST. From the measured values, the visual range (L_v) was calculated using the Koschmieder relationship (ignoring the absorption terms). At the peak of the episode, a greatly reduced visual range of 8.3 km was observed. At background aerosol conditions close to σ_{sp} = 0 Mm^{-1}, the visual range was calculated to be 260 km due to Rayleigh scattering only.

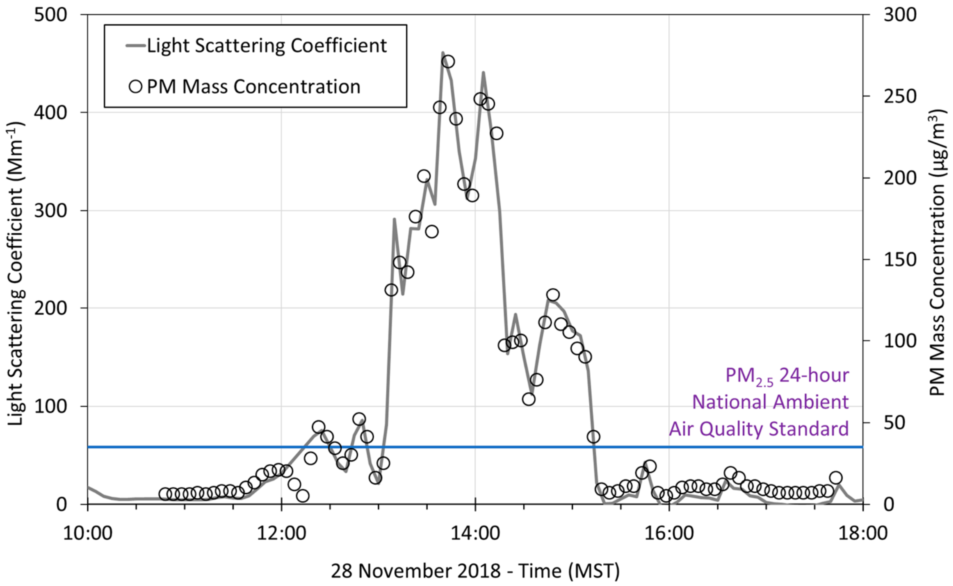

Figure 2. Time Series of 'dry' light scattering coefficient (σ_{sp}) (520 nm) and 'dry' $PM_{2.5}$ mass concentration (μg/m^3).

The measured particulate concentration ranged from ~0 to 270 μg/m^3 as measured with the DustTrak and shown in Figure 2. The 24 h $PM_{2.5}$ National Ambient Air Quality standard, 8 times lower than the peak concentration observed, was also indicated at 35 μg/m^3 for gauging severity. Even with the short nature of the event, the 24 h $PM_{2.5}$ concentration on 28 November 2018 reached 26.6 μg/m^3.

The two instruments tracked very closely during the event as indicated by the high R^2 = 0.97 (Figure 3). This was not surprising given that both methods rely on a light scattering method (although integrated vs. narrow, fixed angle). Taking the slope of the relationship between σ_{sp} and [$PM_{2.5}$] traditionally gives an estimate of the mass scattering efficiency when combining optical and gravimetric methods. A typical range of 2 m^2/g to 6 m^2/g for scattering efficiency was observed for ambient aerosols [33]. The slope here, 1.7 m^2/g, was likely an underestimate of the true efficiency in part due to the DustTrak calibration with respirable ATD and the possible differences in particle transmission efficiency. The mass scattering efficiency decreases for larger diameters but also for very small sizes due to the decreasing scattering efficiency Q_{sp}. For example, a dry organic aerosol provides a mass scattering of ~1.7 m^2/g for an effective D_p ~150 nm [34]. Although this was not an unreasonable assumption for ~1.5-h-old smoke [29], we refrained from quantifying this as a 'true' scattering efficiency.

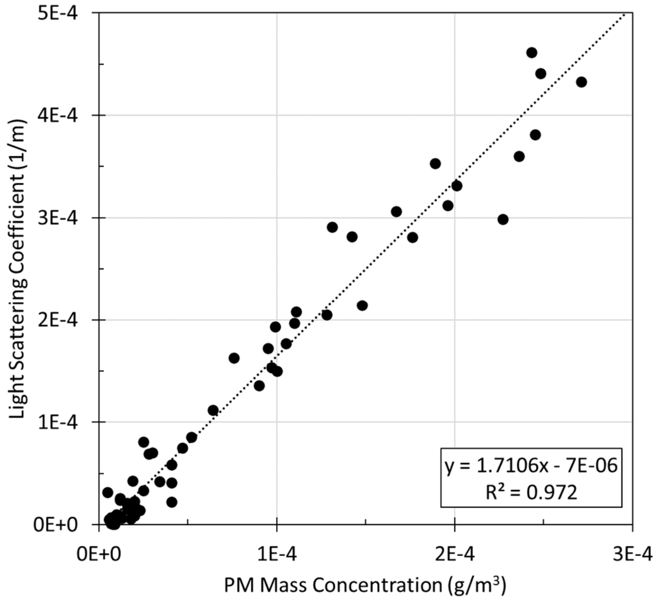

Figure 3. Relationship between light scattering of particles (1/m) and PM mass concentration (g/m^3), which gives a slope in m^2/g.

A summary attribution of the reconstructed light extinction from the 24-h filter sample $PM_{2.5}$ chemical composition on 28 November 2018 at the nearby Bosque del Apache IMPROVE monitoring station (BOAP1) is shown in Figure 4 using standard IMPROVE protocols. The IMPROVE monitor was located at the northwest corner of BOAP and thus was approximately in the flow path from BOAP to the receptor site in Socorro, NM. The apportionment of light extinction was based on the composition analysis of 24-h filter samples using the IMPROVE algorithms. The dominance of organic carbon and secondarily elemental carbon is typical of ambient biomass smoke [7].

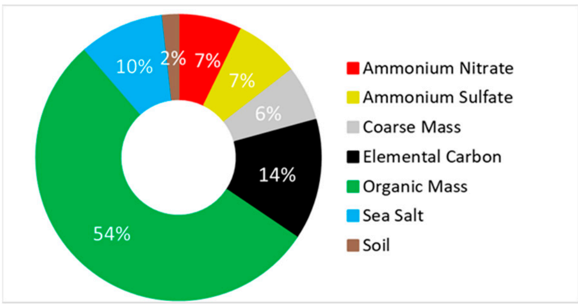

Figure 4. $PM_{2.5}$ contributions to reconstructed light extinction at the Bosque del Apache IMPROVE site (BOAP1) on 28 November 2018.

To understand the general mesoscale atmospheric transport and meteorological context, the back trajectory analysis was run using the NOAA HYSPLIT model (Figure 5). During the smoke event, the sky was cloud-free, the ambient dry-bulb temperature was 14 ± 2 °C (range from 10 to 16 °C), and the pressure was steady at 851 hPa according to the National Weather Service data. The model featured six back trajectories at one-hour intervals arriving at the receptor height of 500 m AGL in Socorro during the event from 11:00 to 16:00 MST as indicated (Figure 5). The meteorological transport featured westerlies with a complex flow around the topography of the Magdalena Mountains to the west of Socorro. The diversion to the south and flow up the Rio Grande Valley was observed in all the trajectories during this period. All modeled back trajectories during the episode showed proximity to BOAP1.

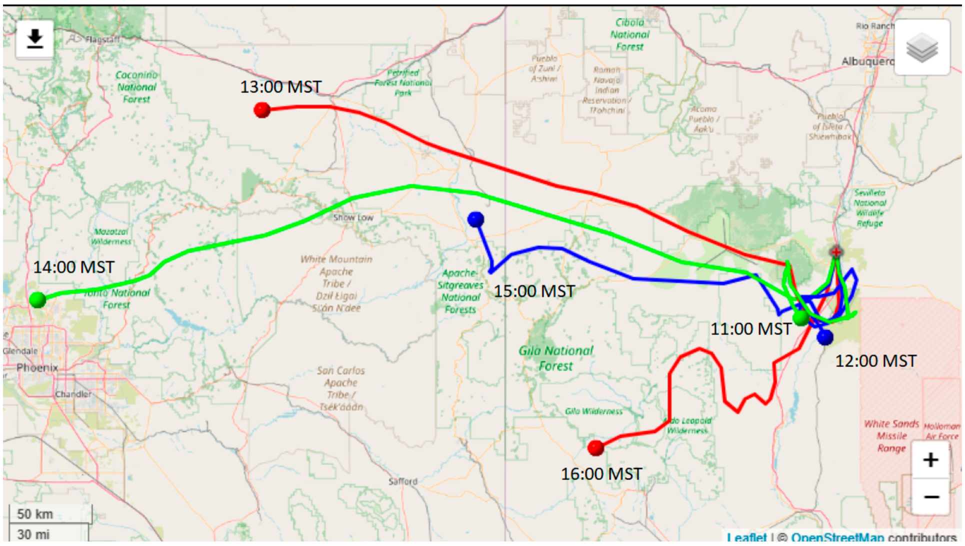

Figure 5. NOAA HYSPLIT model 24-h back trajectories arriving at the receptor site during the smoke episode on 28 November 2018 (six trajectories arriving on the hour from 11:00 to 16:00 MST).

The local wind data for 28 November 2018 are shown in Figures 6 and 7 as a wind rose and time series, respectively. During the hours of the haze event in Socorro, local winds shifted to south-southeast beginning around 10:00 MST. and lasting until approximately 18:00 MST. The transport time was ~1.5 h from the IMPROVE site to the receptor site at windspeeds during the late morning. Elevated $PM_{2.5}$ concentrations followed the wind pattern quite closely, also showing that the local nature of the event was likely confined to the Rio Grande Valley where diurnal up- versus down-slope atmospheric flow occurred. Prescribed fire impacts may be identified due to their discrete, often single-day nature, and isolated due to their small-scale and targeted nature as suggested in other studies [35].

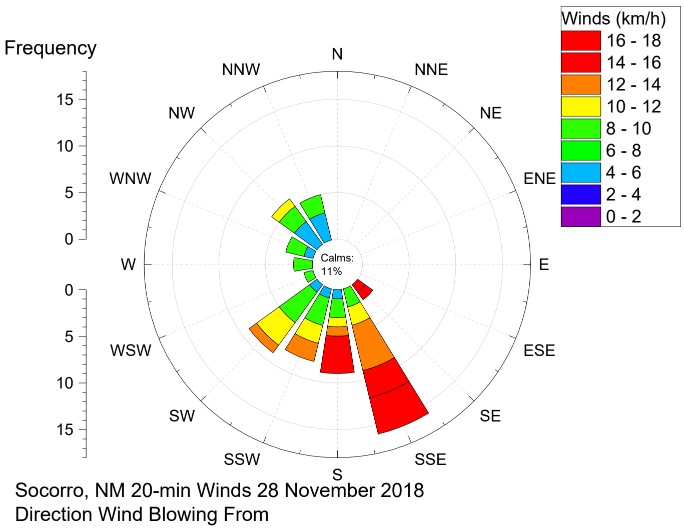

Figure 6. Socorro, New Mexico, surface wind speed and direction data (20 min averages) plotted as a wind rose over 24 h on 28 November 2018.

The Interagency Monitoring Network for Protected Visual Environments (IMPROVE) is a nationwide network of remote sites for monitoring regional aerosol properties in scenic areas including national parks and monuments [36]. We examined IMPROVE data from six sites in NM, and four each in Arizona and Colorado (Table 2). Since none of the sites were co-located with the Socorro site, rather than a quantitative comparison, the data were included to demonstrate the extent and regionality of the event. The nearest station to Socorro was Bosque del Apache (BOAP1), the site of the prescribed fire, and was approximately 17 km south of the Socorro site. BOAP1 and Socorro are both located in the Rio Grande Valley, extending from north to south, from the Rocky Mountains of southern Colorado to the border with Mexico in the south.

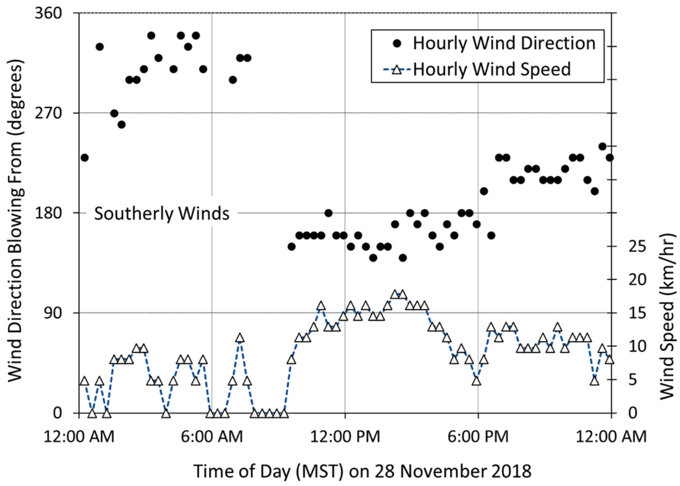

Figure 7. Local wind speed and direction (20 min) plot in Socorro, NM, on 28 November 2018.

Table 2. IMPROVE monitoring site reconstructed 24 h average light extinction coefficient (Mm^{-1}) data for 28 November 2018. NA = Data Not Available.

Class 1 Area	IMPROVE Monitor	Light Extinction (Mm^{-1})
Bandelier Wilderness	BAND1	15.8
Bosque del Apache Wilderness	BOAP1	76.9
Carlsbad Caverns National Park	GUMO1	33.9
Gila Wilderness	GICL1	13.8
Salt Creek Wilderness	SACR1	22.0
San Pedro Parks Wilderness	SAPE1	10.5
Wheeler Peak Wilderness	WHPE1	NA
White Mountain Wilderness	WHIT1	14.5
Petrified Forest National Park (AZ)	PEFO1	16.8
Mount Baldy (AZ)	BALD1	10.8
Chiricahua (AZ)	CHIR1	16.7
Grand Canyon National Park (AZ)	GRCA2	15.2
Shamrock Mine (CO)	SHMI1	14.2
Mesa Verde National Park (CO)	MESA1	13.2
Weminuche Wilderness (CO)	WEMI1	13.4
Great Sand Dunes N.M. (CO)	GRSA1	13.6

The surrounding IMPROVE monitoring site data on 28 November 2018 were examined to assess the regional impact of the event. The measured 24-h σ_{ep} is shown in Table 2 (light extinction coefficients were reconstructed from filter measurements using standard IMPROVE calculations). At the surrounding IMPROVE sites on 28 November 2018, reconstructed light extinction by particles is <34 Mm^{-1} at all sites (and apart from Carlsbad, σ_{ep} < 22 Mm^{-1}), typical of winter background conditions. Bosque del Apache was the lone site in the region that showed such elevated light extinction. The evidence from the surrounding sites on 28 November 2018 showed that the smoke in Socorro was likely driven by more proximate sources.

At BOAP1, the event on 28 November 2018 was the second largest concentration measured with IMPROVE during the year. The reconstructed 24-h $PM_{2.5}$ mass concentration was approximately 50 $\mu g/m^3$ and the composition was dominated by organic carbon with a secondary contribution from elemental carbon as discussed earlier. Such is typical with ambient smoke events [7]. The reconstructed 24-h σ_{ext} during this event was approximately 77 Mm^{-1} at BOAP1. As expected, due to dilution, particle loss, plus no light absorption information, the downwind Socorro 24-h σ_{sp} of 42 Mm^{-1} was somewhat lower although of a similar magnitude. The confinement of the event to the Rio Grande Valley provided evidence that it was more likely the local prescribed fire occurring that day rather than a regional-scale event. As a frame of reference, during the Whitewater-Baldy wildfire in 2012 (not shown), smoke impacts persisted for approximately 2 weeks with maximum 24-h reconstructed light extinction of 300 Mm^{-1} at BOAP1.

The NASA Fire Information for Resource Management System (FIRMS) integrates multiple satellite detections of fire hotspots. As viewed with NASA FIRMS, the fire activity was light during this period and included a few small fires in Arizona and New Mexico (Figure 8). The prescribed fire detected at BOAP1 between Albuquerque and White Sands Missile Range is shown in the circle south of the sampling site. Although outside the wildfire season, contributions from the other small, indicated fires in Arizona and New Mexico were possible (small red fire detection areas west of the sampling site in Figure 8).

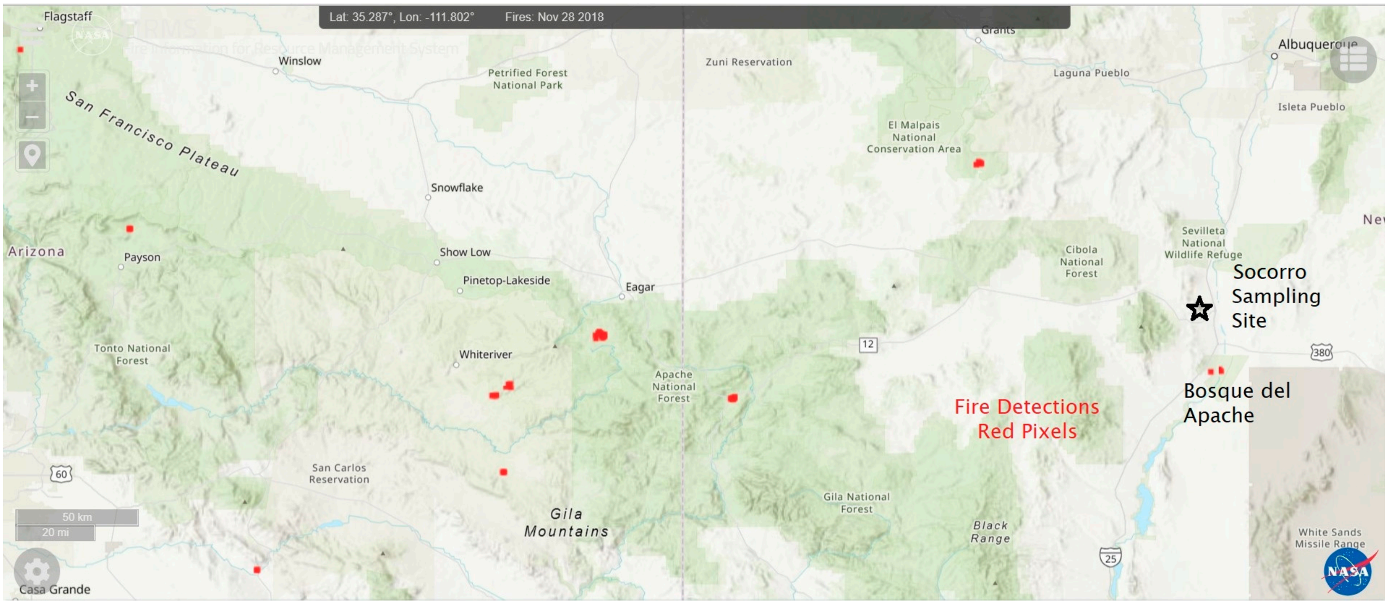

Figure 8. NASA FIRMS satellite data on regional fire detection hotspots in the upwind direction from Socorro, NM (circled receptor site) on 28 November 2018. The prescribed fire satellite detected burn areas (red areas) are shown in the circled area to the south of the Socorro site.

4. Conclusions

A large magnitude, though short in duration, haze event with severely degraded air quality occurred in Socorro, NM, on the afternoon of 28 November 2018. With the data presented herein, the impacts were driven primarily by biomass smoke from a prescribed burn located at the Bosque del Apache near San Antonio, New Mexico. The smoke caused a significant reduction in visibility, with an extinction coefficient (5 min average) maximum of 470 Mm^{-1} limiting the visual range to <8.3 km at the event peak. No other nearby monitoring stations showed a clear perturbation above the typically observed background concentrations. Local wind data, paired with back trajectory analysis using the NOAA HYSPLIT model, suggested transport impacts from a proximate prescribed fire at Bosque del Apache wildlife refuge. The increasing use of prescribed burning, a vital tool for ecosystem management to mitigate wildfire frequency and severity, will likely lead to more conflicts between the former goals and maintaining air quality. This study represents only a snapshot of the magnitude of the unintended impacts of a discrete prescribed fire event.

Further measurements and modeling are required to fully understand the extensive and intensive properties of prescribed fire smoke and how impacts can be mitigated.

Author Contributions: Conceptualization, C.M.C.; methodology, C.M.C.; validation, C.M.C.; formal analysis, J.K.; data curation, J.K. and C.M.C.; writing—original draft preparation, J.K.; writing—review and editing, C.M.C.; visualization, C.M.C. and J.K.; supervision, C.M.C.; project administration, C.M.C.; funding acquisition, C.M.C. All authors have read and agreed to the published version of the manuscript.

Funding: This material is part based upon work supported by the National Science Foundation under Grant No. 1832813. This work was supported in part by the U.S. Department of Energy, Office of Science, Office of Workforce Development for Teachers and Scientists (WDTS) under the Visiting Faculty Program (VFP), and the DOE Student Undergraduate Laboratory Intern Program. The New Mexico Consortium is gratefully acknowledged for financial support of this research.

Institutional Review Board Statement: Not applicable.

Informed Consent Statement: Not applicable.

Data Availability Statement: Data are available by emailing the corresponding author.

Acknowledgments: The authors gratefully acknowledge the reviews of four anonymous referees whose input improved the manuscript. We also acknowledge the NOAA Air Resources Laboratory (ARL) for the provision of the HYSPLIT transport and dispersion model and the READY website (https://www.ready.noaa.gov, accessed on 20 December 2022) used in this publication. We acknowledge the use of data and imagery from NASA's Fire Information for Resource Management System (FIRMS) (https://earthdata.nasa.gov/firms, accessed on 20 December 2022), part of NASA's Earth Observing System Data and Information System (EOSDIS). The authors also acknowledge OpenStreetMap and its contributors for the provision of the OpenStreetMap base map and associated data licensed under the Open Data Commons Open Database License (ODbL) by the OpenStreetMap Foundation (OSMF). We acknowledge the IMPROVE network data for contextual data and insight provided. IMPROVE is a collaborative association of state, tribal, and federal agencies, and international partners. The U.S. Environmental Protection Agency is the primary funding source, with contracting and research support from the National Park Service. The Air Quality Group at the University of California, Davis, is the central analytical laboratory, with ion analysis provided by the Research Triangle Institute, and carbon analysis provided by the Desert Research Institute. Data products from the WRAP Technical Support System (TSS); CSU and the Cooperative Institute for Research in the Atmosphere (CIRA), https://views.cira.colostate.edu/tssv2, accessed on 19 December 2022, were used. The authors also acknowledge Carrico's Fall 2018 Air Resources Engineering students who aided in the collection of the data presented herein.

Conflicts of Interest: The authors declare no conflict of interest.

References

1. Jaffe, D.A.; O'Neill, S.M.; Larkin, N.K.; Holder, A.L.; Peterson, D.L.; Halofsky, J.E.; Rappold, A.G. Wildfire and prescribed burning impacts on air quality in the United States. *J. Air Waste Manag. Assoc.* **2020**, *70*, 583–615. [CrossRef] [PubMed]
2. Altshuler, S.L.; Zhang, Q.; Kleinman, M.T.; Garcia-Menendez, F.; Moore, C.T.; Hough, M.L.; Stevenson, E.D.; Chow, J.C.; Jaffe, D.A.; Watson, J.G. Wildfire and prescribed burning impacts on air quality in the United States. *J. Air Waste Manag. Assoc.* **2020**, *70*, 961–970. [CrossRef] [PubMed]
3. Westerling, A.; Hidalgo, H.; Cayan, D.; Swetnam, T. Warming and earlier spring increase western US forest wildfire activity. *Science* **2006**, *313*, 940–943. [CrossRef]
4. Abatzoglou, J.T.; Williams, A.P. Impact of anthropogenic climate change on wildfire across western US forests. *Proc. Natl. Acad. Sci. USA* **2016**, *113*, 11770–11775. [CrossRef]
5. Elahi, E.; Khalid, Z.; Tauni, M.Z.; Zhang, H.; Lirong, X. Extreme weather events risk to crop-production and the adaptation of innovative management strategies to mitigate the risk: A retrospective survey of rural Punjab, Pakistan. *Technovation* **2022**, *117*, 102255. [CrossRef]
6. Bowman, D.; Kolden, C.A.; Abatzoglou, J.T.; Johnston, F.H.; van der Werf, G.R.; Flannigan, M. Vegetation fires in the Anthropocene. *Nat. Rev. Earth Environ.* **2020**, *1*, 500–515. [CrossRef]
7. McMeeking, G.; Kreidenweis, S.; Carrico, C.; Lee, T.; Collett, J.; Malm, W. Observations of smoke-influenced aerosol during the Yosemite Aerosol Characterization Study: Size distributions and chemical composition. *J. Geophys. Res. Atmos.* **2005**, *110*. [CrossRef]

8. Naeher, L.P.; Brauer, M.; Lipsett, M.; Zelikoff, J.T.; Simpson, C.D.; Koenig, J.Q.; Smith, K.R. Woodsmoke health effects: A review. *Inhal. Toxicol.* **2007**, *19*, 67–106. [CrossRef]
9. Malm, W.C.; Sisler, J.F.; Huffman, D.; Eldred, R.A.; Cahill, T.A. Spatial and Seasonal Trends in Particle Concentration and Optical Extinction in the United States. *J. Geophys. Res. Atmos.* **1994**, *99*, 1347–1370. [CrossRef]
10. IPCC. Climate Change 2021: The Physical Science Basis. In *Contribution of Working Group I to the Sixth Assessment Report of the Intergovernmental Panel on Climate Change*; Masson-Delmotte, V., Zhai, P., Pirani, A., Connors, S., Péan, C., Berger, S., Caud, N., Chen, Y., Goldfarb, L., Gomis, M., Huang, M., Leitzell, K., Lonnoy, E., Matthews, J., Maycock, T., Waterfield, T., Yelekçi, O., Yu, R., Zhou, B., Eds.; Cambridge University Press: Cambridge, UK; New York, NY, USA, 2021.
11. Ryan, K.C.; Knapp, E.E.; Varner, J.M. Prescribed fire in North American forests and woodlands: History, current practice, and challenges. *Front. Ecol. Environ.* **2013**, *11*, E15–E24. [CrossRef]
12. Schoennagel, T.; Balch, J.K.; Brenkert-Smith, H.; Dennison, P.E.; Harvey, B.J.; Krawchuk, M.A.; Mietkiewicz, N.; Morgan, P.; Moritz, M.A.; Rasker, R.; et al. Adapt to more wildfire in western North American forests as climate changes. *Proc. Natl. Acad. Sci. USA* **2017**, *114*, 4582–4590. [CrossRef]
13. Andreae, M.O.; Merlet, P. Emission of trace gases and aerosols from biomass burning. *Glob. Biogeochem. Cycles* **2001**, *15*, 955–966. [CrossRef]
14. McMeeking, G.; Kreidenweis, S.; Baker, S.; Carrico, C.; Chow, J.; Collett, J.; Hao, W.; Holden, A.; Kirchstetter, T.; Malm, W.; et al. Emissions of trace gases and aerosols during the open combustion of biomass in the laboratory. *J. Geophys. Res. Atmos.* **2009**, *114*. [CrossRef]
15. Bond, T.C.; Doherty, S.J.; Fahey, D.W.; Forster, P.M.; Berntsen, T.; DeAngelo, B.J.; Flanner, M.G.; Ghan, S.; Karcher, B.; Koch, D.; et al. Bounding the role of black carbon in the climate system: A scientific assessment. *J. Geophys. Res. Atmos.* **2013**, *118*, 5380–5552. [CrossRef]
16. Gomez, S.; Carrico, C.; Allen, C.; Lam, J.; Dabli, S.; Sullivan, A.; Aiken, A.; Rahn, T.; Romonosky, D.; Chylek, P.; et al. Southwestern US Biomass Burning Smoke Hygroscopicity: The Role of Plant Phenology, Chemical Composition, and Combustion Properties. *J. Geophys. Res. Atmos.* **2018**, *123*, 5416–5432. [CrossRef]
17. Liu, Y.Q.; Goodrick, S.; Heilman, W. Wildland fire emissions, carbon, and climate: Wildfire-climate interactions. *For. Ecol. Manag.* **2014**, *317*, 80–96. [CrossRef]
18. Rocca, M.E.; Brown, P.M.; MacDonald, L.H.; Carrico, C.M. Climate change impacts on fire regimes and key ecosystem services in Rocky Mountain forests. *For. Ecol. Manag.* **2014**, *327*, 290–305. [CrossRef]
19. Nelson, J.; Chalbot, M.C.G.; Tsiodra, I.; Mihalopoulos, N.; Kavouras, I.G. Physicochemical Characterization of Personal Exposures to Smoke Aerosol and PAHs of Wildland Firefighters in Prescribed Fires. *Expo. Health* **2021**, *13*, 105–118. [CrossRef]
20. Price, O.F.; Horsey, B.; Jiang, N.B. Local and regional smoke impacts from prescribed fires. *Nat. Hazards Earth Syst. Sci.* **2016**, *16*, 2247–2257. [CrossRef]
21. Lee, S.; Kim, H.K.; Yan, B.; Cobb, C.E.; Hennigan, C.; Nichols, S.; Chamber, M.; Edgerton, E.S.; Jansen, J.J.; Hu, Y.T.; et al. Diagnosis of aged prescribed burning plumes impacting an urban area. *Environ. Sci. Technol.* **2008**, *42*, 1438–1444. [CrossRef]
22. Liu, X.X.; Huey, L.G.; Yokelson, R.J.; Selimovic, V.; Simpson, I.J.; Muller, M.; Jimenez, J.L.; Campuzano-Jost, P.; Beyersdorf, A.J.; Blake, D.R.; et al. Airborne measurements of western US wildfire emissions: Comparison with prescribed burning and air quality implications. *J. Geophys. Res. Atmos.* **2017**, *122*, 6108–6129. [CrossRef]
23. Burling, I.R.; Yokelson, R.J.; Akagi, S.K.; Urbanski, S.P.; Wold, C.E.; Griffith, D.W.T.; Johnson, T.J.; Reardon, J.; Weise, D.R. Airborne and ground-based measurements of the trace gases and particles emitted by prescribed fires in the United States. *Atmos. Chem. Phys.* **2011**, *11*, 12197–12216. [CrossRef]
24. Sullivan, A.; May, A.; Lee, T.; McMeeking, G.; Kreidenweis, S.; Akagi, S.; Yokelson, R.; Urbanski, S.; Collett, J. Airborne characterization of smoke marker ratios from prescribed burning. *Atmos. Chem. Phys.* **2014**, *14*, 10535–10545. [CrossRef]
25. Hodshire, A.L.; Bian, Q.; Ramnarine, E.; Lonsdale, C.R.; Alvarado, M.J.; Kreidenweis, S.M.; Jathar, S.H.; Pierce, J.R. More Than Emissions and Chemistry: Fire Size, Dilution, and Background Aerosol Also Greatly Influence Near-Field Biomass Burning Aerosol Aging. *J. Geophys. Res. Atmos.* **2019**, *124*, 5589–5611. [CrossRef]
26. Hodshire, A.L.; Ramnarine, E.; Akherati, A.; Alvarado, M.L.; Farmer, D.K.; Jathar, S.H.; Kreidenweis, S.M.; Lonsdale, C.R.; Onasch, T.B.; Springston, S.R.; et al. Dilution impacts on smoke aging: Evidence in Biomass Burning Observation Project (BBOP) data. *Atmos. Chem. Phys.* **2021**, *21*, 6839–6855. [CrossRef]
27. May, A.A.; Lee, T.; McMeeking, G.R.; Akagi, S.; Sullivan, A.P.; Urbanski, S.; Yokelson, R.J.; Kreidenweis, S.M. Observations and analysis of organic aerosol evolution in some prescribed fire smoke plumes. *Atmos. Chem. Phys.* **2015**, *15*, 6323–6335. [CrossRef]
28. Levin, E.; McMeeking, G.; Carrico, C.; Mack, L.; Kreidenweis, S.; Wold, C.; Moosmuller, H.; Arnott, W.; Hao, W.; Collett, J.; et al. Biomass burning smoke aerosol properties measured during Fire Laboratory at Missoula Experiments (FLAME). *J. Geophys. Res. Atmos.* **2010**, *115*. [CrossRef]
29. Carrico, C.; Prenni, A.; Kreidenweis, S.; Levin, E.; McCluskey, C.; DeMott, P.; McMeeking, G.; Nakao, S.; Stockwell, C.; Yokelson, R. Rapidly evolving ultrafine and fine mode biomass smoke physical properties: Comparing laboratory and field results. *J. Geophys. Res. Atmos.* **2016**, *121*, 5750–5768. [CrossRef]
30. Carrico, C.M.; Capek, T.J.; Gorkowski, K.J.; Lam, J.T.; Gulick, S.; Karacaoglu, J.; Lee, J.E.; Dungana, C.; Aiken, A.C.; Onasch, T.B.; et al. Humidified single-scattering albedometer (H-CAPS-PMSSA): Design, data analysis, and validation. *Aerosol Sci. Technol.* **2021**, *55*, 749–768. [CrossRef]

31. Stein, A.; Draxler, R.; Rolph, G.; Stunder, B.; Cohen, M.; Ngan, F. NOAA'S HYSPLIT Atmospheric Transport and Dispersion Modeling System. *Bull. Am. Meteorol. Soc.* **2015**, *96*, 2059–2077. [CrossRef]
32. Rolph, G.D. *Real-Time Environmental Applications and Display sYstem (READY)*; NOAA Air Resources Laboratory: College Park, MD, USA, 2017. Available online: http://www.ready.noaa.gov (accessed on 19 December 2022).
33. Hand, J.; Malm, W. Review of aerosol mass scattering efficiencies from ground-based measurements since 1990. *J. Geophys. Res. Atmos.* **2007**, *112*. [CrossRef]
34. Latimer, R.N.C.; Martin, R.V. Interpretation of measured aerosol mass scattering efficiency over North America using a chemical transport model. *Atmos. Chem. Phys.* **2019**, *19*, 2635–2653. [CrossRef]
35. Huff, A.K.; Kondragunta, S.; Zhang, H.; Laszlo, I.; Zhou, M.; Caicedo, V.; Delgado, R.; Levy, R. Tracking Smoke from a Prescribed Fire and Its Impacts on Local Air Quality Using Temporally Resolved GOES-16 ABI Aerosol Optical Depth (AOD). *J. Atmos. Ocean. Technol.* **2021**, *38*, 963–976. [CrossRef]
36. Malm, W.C. *Introduction to Visibility*; U.S. National Park Service: Fort Collins, CO, USA, 1999; p. 70.